

Morphometric Study of The Ventricular Indexes in Healthy Ovine Brain Using MRI

Marco Trovati

Università degli Studi di Milano <https://orcid.org/0000-0003-2413-9499>

Carlotta Spediacci

Università degli Studi di Milano

Antonella Castellano

Università Vita Salute San Raffaele

Andrea Bernardini

Imperial College London

Daniele Dini

Imperial College London

Luca Malfassi

Fondazione La Cittadina Studi e Ricerche Veterinarie

Valentina Pieri

Università Vita Salute San Raffaele

Andrea Falini

Università Vita Salute San Raffaele

Giuliano Ravasio

Università degli Studi di Milano

Marco Riva

Università degli Studi di Milano

Lorenzo Bello

Università degli Studi di Milano

Stefano Brizzola

Università degli Studi di Milano

Davide Danilo Zani (✉ davide.zani@unimi.it)

Università degli Studi di Milano

Research article

Keywords: Anatomy, Imaging, Sheep, Brain, MRI

Posted Date: August 12th, 2020

DOI: <https://doi.org/10.21203/rs.3.rs-51715/v1>

License: © ⓘ This work is licensed under a Creative Commons Attribution 4.0 International License. [Read Full License](#)

Version of Record: A version of this preprint was published at BMC Veterinary Research on March 11th, 2022. See the published version at <https://doi.org/10.1186/s12917-022-03180-0>.

Abstract

Background

Sheep (*Ovis aries*) have been largely used as animal models in a multitude of specialties in biomedical research. The similarity to human brain anatomy in terms of brain size, skull features, and gyrification index, gives to ovine as a large animal model a better translational value than small animal models in neuroscience. Despite this evidence and the availability of advanced imaging techniques, morphometric brain studies are lacking. We herein present the morphometric ovine brain indexes and anatomical measures developed by two observers in a double-blinded study and validated via an intra- and inter-observer analysis.

Results

For this retrospective study, T1-weighted Magnetic Resonance Imaging (MRI) scans were performed at 1.5T on 15 sheep, under general anaesthesia. The animals were female *Ovis aries*, in the age of 18-24 months. Two observers assessed the scans, twice time each. The statistical analysis of intra-observer and inter-observer agreement was obtained via the Bland-Altman plot and Spearman rank correlation test.

The results are as follows (mean±Standard deviation):

Indexes: Bifrontal $0,338 \pm 0,032$ cm; Bicaudate $0,080 \pm 0,012$ cm; Evans' $0,218 \pm 0,035$ cm; Ventricular $0,241 \pm 0,039$ cm; Huckman $1,693 \pm 0,174$ cm; Cella Media $0,096 \pm 0,037$ cm; Third ventricle ratio $0,040 \pm 0,007$ cm.

Anatomical measures: Fourth ventricle length $0,295 \pm 0,073$ cm; Fourth ventricle width $0,344 \pm 0,074$ cm; Left lateral ventricle $4,175 \pm 0,275$ cm; Right lateral ventricle $4,182 \pm 0,269$ cm; Frontal horn length $1,795 \pm 0,303$ cm; Interventricular foramen left $1,794 \pm 0,301$ cm; Interventricular foramen right $1,78 \pm 0,317$ cm.

Conclusions

The present study provides baseline values of linear indexes of the ventricles in the ovine models. The acquisition of these data contributes to filling the knowledge void on important anatomical and morphological features of the sheep brain.

Background

Sheep have been largely used in preclinical research as large animal models, due to the anatomical and morphological similarities between the ovine and the human brain.

In order to follow the 3R rules(1) and obtain the best translational value, large animal models are better models than small animals in the neuroscientific research. Small animal models, such as mouse, rat, and rabbit, are usually preferred due to the low cost, ease of care, and the possibility of a high work rate. While they are still valuable for addressing basic research questions, the translation of therapeutic approaches from bench to bed side is often inadequate. Thus, there is a growing awareness that therapies should be tested in large-animal models before clinical application(2). Limitations of the small animal models are related to anatomical features. A smooth and lissencephalic neocortex characterizes murine models. Accordingly, their gyrification index (GI) -defined as the ratio of total neocortical surface area, including sulci, to superficially exposed neocortical surface area- has a rate of 1.00. Rabbit is counted among the lissencephalic brain type in contrast to the gyrencephalic one and it is

characterized by a GI of 1.2(3). Humans exhibit a GI of 2.56 that is more than twice the value of the small animal models.

Despite the extensive use of ovine in the biomedical research and the availability of advanced diagnostic imaging techniques such as computed tomography (CT)(4), magnetic resonance imaging (MRI) (5) with diffusion tensor imaging studies (DTI)(6), morphometric brain studies are still lacking. Sheep have been mostly studied from a functional point of view, and a cortical map has been created identifying different areas like motor and sensory areas as in humans. These morphofunctional properties were investigated from structural points. A tractography atlas with the principal white matter fibre bundles was built(6).

Morphometric study of the brain ventricles is commonly used in clinics, since it is a valuable radiological tool for the diagnosis and classification of hydrocephalus or monitoring procedures, such as ventricular shunting. Therefore, the morphometric characteristics of the ovine brain could be a useful reference tool for improving the quality of the research in scientific scenarios, according to the fundamental 3R rules for animal model usage.

Considering this relevant contribution to the scientific community, sheep still lack morphometric data and a comprehensive description of their brain size indexes, thus missing relevant parameters for anatomical arguments. Thorough knowledge of these morphometric features is essential to create an anatomical database for planning research based on sheep as experimental models.

This study aims to establish normal values for bifrontal, bicaudate, ventricular, Huckman's, Evans's, third ventricular and cella media index in sheep. Anatomical measures of fourth ventricle length and width, left and right lateral ventricle, frontal horn length, left and right Interventricular foramen have also been assessed.

Results

The results of each value are reported in Table 1.

The value of Bifrontal index is $0,338 \pm 0,032$ cm. The value is calculated as the maximum distance between anterior horns divided by the maximum internal diameter of frontal bone.

The Bicaudate index is $0,080 \pm 0,012$ cm. This index is calculated as the minimum bicaudate nuclei distance divided by the maximum distance between anterior horns.

Evans' index is $0,218 \pm 0,035$ cm. This index is calculated as the maximum distance between anterior horns divided by the maximum internal skull diameter.

Ventricular index value is $0,241 \pm 0,035$ cm. This value is the sum of minimum width of the lateral ventricle and the maximum bifrontal diameter.

Huckman index results in $1,693 \pm 0,174$ cm. This value is a measure related to the diameter of anterior ventricular horn. This index is calculated by adding the maximum distance between anterior horns and the minimum bicaudate nuclei distance.

Cella media results in $0,096 \pm 0,037$ cm. This value is calculated as the ratio of the width of cella media and the maximum inner skull diameter.

Third ventricle index shows is $0,040 \pm 0,007$ cm. This ratio is calculated between the third ventricle lateral margin and the transverse diameter of the brain, measured along the same line.

Table 1
Ventricular indexes of the healthy adult ovine. The main brain indexes are reported with mean and standard deviation

Ventricular index	Mean	Standard Deviation
Bifrontal	0,338	$\pm 0,032$
Bicaudate	0,080	$\pm 0,012$
Evans	0,218	$\pm 0,035$
Ventricular	0,241	$\pm 0,039$
Huckman	1,693	$\pm 0,174$
Cella Media	0,096	$\pm 0,037$
Third ventricle ratio	0,040	$\pm 0,007$

In addition to the indexes reported as different ratios, Table 2 reports the results as anatomical measures

Table 2
Ventricular measures of healthy adult ovine, reported with mean and standard deviation

Ventricular measure	Mean	Standard Deviation
Fourth ventricle length	0,295	$\pm 0,073$
Fourth ventricle width	0,344	$\pm 0,074$
Left lateral ventricle	4,175	$\pm 0,275$
Right lateral ventricle	4,182	$\pm 0,269$
Frontal horn length	1,795	$\pm 0,303$
Interventricular foramen left	1,794	$\pm 0,301$
Interventricular foramen right	1,780	$\pm 0,317$

Tables with the resuming values of the Bland-Altman plots (average bias and limits of agreement) and the Spearman's rank correlation results (ρ and corresponding p-value) are herein presented. Here, the 'bias' is the difference between each pair of measurements, while the 'limits of agreement' define the acceptable interval around the average bias. In all Bland-Altman plots, for both the inter and intra-observer variability investigations, more than 95% of the data points lie within the calculated limits of agreement. The complete set of the Bland-Altman are provided in the Supplementary Information.

Inter-observer variability comparing Bland-Altman plot between A_1 time and B_1 time shows perfect agreement between the two observers (Table 3). A clinically small bias, always close to 0, indicates that there is strong agreement between the measurements recorded by the two observers. In the first repetition, there is a complete agreement over all the quantities measured.

Table 3
Mean bias and the limits of agreement per each Bland-Altman in inter-observer variability time1

Quantity	Lower Limit Agreement	Bias	Upper Limit Agreement	Spearman Rho	P-Value	Corr(Diff/Mean)	Agreement
Bicaudate	-0,0157	-9,15E-04	0,0138	0,0964	0,7337	□	✓
Bifrontal	-0,0287	0,0267	0,0821	-0,0321	0,9132	□	✓
Cella media	-0,0203	0,012	0,0443	-0,4	0,1408	□	✓
Evans	-0,0187	0,0249	0,0685	-0,5036	0,0582	□	✓
Interventricular foramen right [cm]	-0,8841	-0,2287	0,4273	-0,1071	0,7048	□	✓
Interventricular foramen left [cm]	-0,8065	-0,2427	0,3212	0,2129	0,4462	□	✓
Fourth ventricle width [cm]	-0,0766	0,0616	0,1998	-0,2821	0,3074	□	✓
Fourth ventricle length [cm]	-0,1906	0,0539	0,2984	-0,0857	0,763	□	✓
Huckmans	-0,1785	0,139	0,4565	-0,4415	0,0995	□	✓
Frontal horn length[cm]	-0,8268	-0,246	0,3348	0,1107	0,6953	□	✓
Third ventricle ratio	-0,0095	0,0072	0,0119	0,2571	0,3538	□	✓
Left lateral ventricle [cm]	-0,7137	-0,1567	0,4003	-0,371	0,1734	□	✓
Right lateral ventricle [cm]	-0,5946	-0,09	0,4146	-0,4236	0,1156	□	✓
Ventricular	-0,0791	-0,0276	0,024	-0,0929	0,7435	□	✓

In the second repetition, most of the measurements agree between the two observers. Non-agreement is exclusively found among the cella media, left frontal horn, right lateral ventricular and ventricular values (Table 4).

Table 4
Mean bias and the limits of agreement per each Bland-Altman in inter-observer variability time 2

Quantity	Lower Limit Agreement	Bias	Upper Limit Agreement	Spearman Rho	P-Value	Corr(Diff/Mean)	Agreement
Bicaudate	-0,0157	-6,00E-04	0,0145	-0,2768	0,3138	∅	✓
Bifrontal	-0,023	0,0277	0,0783	-0,4	0,14	∅	✓
Cellamedia	-0,0127	0,0292	0,0711	0,6179	0,0163	∅	✓
Evans	-0,062	0,0513	0,1646	0,3321	0,2264	∅	✓
Interventricular foramen right [cm]	-0,9394	-0,47	-6,01E-04	0,4093	0,1298	∅	✓
Interventricular foramen left [cm]	-0,9745	-0,4753	0,0239	0,4714	0,0783	∅	✓
Fourth ventricle width [cm]	-0,0931	0,0389	0,1708	0,3807	0,1615	∅	✓
Fourth ventricle length [cm]	-0,1293	0,0203	0,1698	0,1698	0,5452	∅	✓
Huckmans	-0,1078	0,1829	0,4737	0,0536	0,8525	∅	✓
Frontal horn length[cm]	-0,9664	-0,478	0,0104	0,588	0,0211	✓	∅
Third ventricle ratio	-0,0096	0,0053	0,0202	0,1821	0,5151	∅	✓
Left lateral ventricle [cm]	-0,4017	-0,0227	0,3563	-0,4826	0,0685	∅	✓
Right lateral ventricle [cm]	-0,3844	0,0167	0,4178	-0,6434	0,0097	✓	∅
Ventricular	-0,1	-0,0382	0,0236	-0,6607	0,009	✓	∅

The intra-observer variability has been checked for observer A in two different time points (Table 5). The data show a strong agreement in all the values except for Bicaudate. Although the average bias of the Bicaudate is significantly small, its Bland-Altman plot shows a slight trend confirmed by the Spearman's ρ and its p-value slightly under the threshold of 0.05.

Table 5
Mean bias and the limits of agreement per each Bland-Altman in intra-observer variability observer A

Quantity	Lower Limit Agreement	Bias	Upper Limit Agreement	Spearman Rho	P-Value	Corr(Diff/Mean)	Agreement
Bicaudate	-0,0114	4,28E-04	0,0123	0,525	0,0471	✓	☐
Bifrontal	-0,0342	-0,0048	0,0245	-0,0857	0,763	☐	✓
Cella media	-0,0462	-3,02E-04	0,0456	0,1286	0,6482	☐	✓
Evans	-0,1057	-0,0123	0,0811	-0,4679	0,0809	☐	✓
Interventricular foramen right [cm]	-0,1913	0,044	2,79E-01	0,3703	0,1743	☐	✓
Interventricular foramen left [cm]	-0,1195	0,0787	0,2769	0,4525	0,0903	☐	✓
Fourth ventricle width [cm]	-0,0931	0,0257	0,1444	-0,3843	0,1573	☐	✓
Fourth ventricle length [cm]	-0,1336	0,0162	0,166	0,22	0,4307	☐	✓
Huckmans	-0,0828	0,0421	0,1669	-0,1036	0,7144	☐	✓
Frontal horn length[cm]	-0,1195	0,0787	0,2769	0,4525	0,0903	☐	✓
Third ventricle ratio	-0,0154	0,0017	0,0066	0,425	0,1159	☐	✓
Left lateral ventricle [cm]	-0,5988	-0,1993	0,2002	0,479	0,0708	☐	✓
Right lateral ventricle [cm]	-0,5919	-0,1447	0,3026	0,3107	0,2592	☐	✓
Ventricular	-0,0323	-0,0031	0,0262	0,3929	0,1485	☐	✓

Also the intra-observer variability for observer B has been checked in two different time points. The data shows disagreement for cella media, interventricular right foramen and horn length values (Table 6). Although the average bias is relatively small for all these quantities, small trends in the non-agreeing quantities can be seen in the Bland-Altman plots and confirmed by the Spearman's rank correlation test.

Table 6

Mean bias and the limits of agreement per each Bland-Altman in intra-observer variability observer B

Quantity	Lower Limit Agreement	Bias	Upper Limit Agreement	Spearman Rho	P-Value	Corr(Diff/Mean)	Agreement
Bicaudate	-0,0151	7,43E-04	0,0166	0,0571	0,8425	∅	∅
Bifrontal	-0,0527	-0,0039	0,0449	-0,1214	0,6669	∅	✓
Cella media	-0,0501	1,69E-02	0,0839	0,8929	0	✓	∅
Evans	-0,0393	0,0142	0,0676	0,4821	0,0711	∅	✓
Interventricular foramen right [cm]	-0,7982	-0,1973	4,04E-01	0,7138	0,0028	✓	∅
Interventricular foramen left [cm]	-0,5486	-0,154	0,2406	0,3643	0,1824	∅	✓
Fourth ventricle width [cm]	-0,108	0,0029	0,1139	0,3393	0,216	∅	✓
Fourth ventricle length [cm]	-0,2097	-0,0175	0,1748	0,395	0,1451	∅	✓
Huckmans	-0,2788	0,086	0,4508	0,42	0,1191	∅	✓
Frontal horn length[cm]	-0,5372	0,1533	0,2306	0,529	0,0426	✓	∅
Third ventricle ratio	-0,0107	-1,89E-04	0,0103	0,2393	0,3892	∅	✓
Left lateral ventricle [cm]	-0,515	-0,0653	0,3844	0,449	0,0932	∅	✓
Right lateral ventricle [cm]	-0,5173	-0,038	0,4413	0,2829	0,3069	∅	✓
Ventricular	-0,1009	-0,0137	0,0736	-0,25	0,3677	∅	✓

Overall, the intra- and inter-observer variability results limited. For all values, the differences in the measurements consistently lies within the limits of agreement. In both the inter- and intra-observer studies, the Spearman's rank correlation tests conclude that for all values, with the few aforementioned exceptions, no correlation is found between the differences of the paired measures and their mean; no proportionate bias is thus recorded.

These analyses show good measure agreement between the two observers, low inter-observer variability and, within the observers, low intra-observer variability, across multiple measurements at different time points. Therefore, the precision, goodness and reliability of the measured quantities can be cleared as acceptable and consistent.

Discussion

Due to their particular anatomy and size, sheep (*Ovis aries*) have been largely used as animal models in a multitude of specialities in biomedical research ranging from orthopaedics(9), traumatic brain injury(10) and neurological disorders(11).

In terms of neuroanatomical correspondences, sheep exhibit some overlapping features with the human regarding electroencephalographic elements(12), neuroradiological features(13), neurovascular structures (14). Skull anatomy is also similar to humans in terms of thickness, porosity and the curvature of the calvarium(15).

Considering these characteristics, cadaveric sheep brains have been used as teaching material for mammalian cerebral anatomy(16) and several neurosurgical techniques have been developed and tested through this neurosurgical animal model(17).

Currently, ovine is a reliable large animal model for the study of different human pathologies with reports of cerebral neurodegeneration, neuroinflammation, and intracellular accumulation of storage bodies containing specific proteins(4). All these pathologies require neuroimaging techniques, such as MRI and CT, to analyse changing in brain size and the ventricular volumes.

In human medicine, ventricular volume is considered the standard measurement of ventricular size. In research studies, a high-quality imaging study paired with volumetric reconstruction is not always feasible and, when it is, it is very time consuming. Additionally, the availability of MRI scanner for large animals is sometimes limited to the high costs and the high level of expertise needed for the large animal model management, such as the procedures for general anaesthesia.

Russel et al(4) reported the third and lateral ventricle volume in sheep. The use of CT, instead of MRI, could limit the discrimination of soft tissue boundaries, with a resulting lower resolution for the ventricle measurements. The intracranial values reported in the manuscript reveal an intracranial volume of 99.9 ± 1.7 ml and a brain volume of 101.1 ± 1.7 ml. Information on volumetric measures are reported, but no mention of linear measurements or indexes, as in our report, has been previously presented until now.

In the current study, MRI was selected instead of CT for its better spatial resolution and soft-tissue discrimination of intracranial structures. MRI proved a reliable measure quality in ventricular dilation and, for this reason, this technique is the commonly chosen method for the study of disorders of the cerebro-spinal fluid, such as hydrocephalus, in both human(18) and animals(19).

The authors acknowledge the specificity of this study as related to a particular age group. In fact, the animals involved in this work are all adult sheep of 18–24 months old. However, no indications about changes in the brain indexes in the sheep are available, but it is reasonable to argue that differences related to age groups can be found, as occur in humans. Russel *et al* (4) reported changes in the sheep brain volume as increments between 3 and 5 months. This modification seems to stop at approximately 9 months, when another growth phase begins until plateauing at about 15 months of age.

Further investigations focused on these volumetric changes over time are needed to further improve the current knowledge on ovine as animal model.

Conclusions

The present study provides reference values of linear indexes of ventricles in the healthy adult ovine animal model. The acquisition of these data with high-field MRI contributes to the knowledge on essential anatomical and morphological features of sheep brain. These indexes represent relevant normative values for many research projects, focused on various neurological and psychiatric disorders associated with ventriculomegaly or neurodegeneration. In conclusion, this study introduces a useful tool that can represent a normative reference for neuroscientists who aim at exploiting sheep as preclinical model.

Methods

Case selection

This is a retrospective study based on 15 MRI scans of female sheep, *ovis aries*, in age of 1–2 years old attending at Veterinary Teaching Hospital, Università degli Studi di Milano. Subjects involved in the study were healthy animals. Therefore, MRI scans of animals undergoing neurosurgical procedures were excluded from the study.

Anaesthesia and Imaging

Animals underwent anaesthesia for the imaging studies, being inducted via intravenous administration of Diazepam 0,25 mg/Kg + Ketamine 5 mg/Kg, intubated and then maintained under general anaesthesia with isoflurane 2% and oxygen 2L/min. They were placed in prone position, with the head located in a be-spoke MRI-compatible headframe (Renishaw®). MR imaging was performed on a 1.5T clinical scanner (Achieva, Philips Healthcare) in a veterinary imaging facility [Fondazione La Cittadina Studi e Ricerche Veterinarie, Romanengo (CR), Italy]. Two small and 2 medium flex coils fixed over both hemispheres were used. The MRI protocol included a T1-weighted volumetric scan for each animal, acquired by using a three-dimensional fast-field-echo (3D-T1 FFE) sequence with the following parameters: TR/TE 25/5 ms; flip angle 40°; voxel size 0.667 × 0.667 × 1.4 mm; SENSE factor R = 2; 150 slices; acquisition time 8 min 40 s.

Dataset preparation

Two observers were recruited for this study. Observer A was a PhD in veterinary science with a veterinary surgery background and Observer B was a PhD student in veterinary science with veterinary radiology background. The observers were double-blinded, and all of the measurements were taken independently by the two, in order to study inter-observer variability. Additionally, the two observers repeated the measurements twice, in order to monitor intra-observer variability as well.

Following the work published by Kolsur *et al.* (20), the acquired images have been analysed to obtain different measures explained below. The indexes calculated was Bifrontal index, Bicaudate index, Evans' index, Ventricular index, Huckman's index, Cella media index, Third ventricle Ratio/index. The indexes were then calculated from values:

A: Maximum bifrontal diameter (Fig. 1)

A1: Brain width (Fig. 1)

B: Lateral ventricles minimum width (Fig. 2)

B1: Brain width (Fig. 2)

C: Maximum inner skull diameter (Fig. 3)

D: Maximum distances between third ventricle lateral margin (Fig. 4)

D1: Brain width measured along line D (Fig. 4)

E: Width of both cella media (Fig. 5)

Statistical analyses

Statistical analyses were performed using Matlab Software (The Mathworks, I. MATLAB and Statistics Toolbox Release 2018b. (2018)). Firstly, descriptive statistics like mean and standard deviations have been calculated. Then, differences in measurements between the two observers (inter-observer variability), and the differences from the same observer in different time points (intra-observer variability) were compared via Bland-Altman plots(7, 8) (Fig. 6). This allowed to check for any discrepancy in the measurements caused by a poor quality of the measurements or by an inadequate imaging procedure that would hinder the creation of a consistent and reliable dataset of these specific anatomical features.

Here, the average bias (average of the differences between each pair of measurements) has been plotted against the mean of the two measurements. Upper and lower limits of agreement are defined around the bias characterised by an interval of 1.96 times the standard deviation of the bias. At least 95% of the data points should lie within these limits. In addition to each Bland-Altman plot, a spearman rank correlation test was performed to check whether there was a relationship between the bias and the mean. When Spearman's ρ approaches 0 with values of $p\text{-value} > 0.05$, it shows that there is not enough evidence to accept the hypothesis of an existing correlation. Therefore, the null hypothesis of no correlation between the mean and the difference of the measurements cannot be rejected. Accordingly, there is no proportionality in the calculated bias, which means that the two measures agree and are equivalent. Finally, when all these conditions are met, then a good agreement between the two measurements is accepted.

Abbreviations

CT: Computed Tomography; DTI: Diffusion Tensor Imaging; GI: Gyrfication Index; MRI: Magnetic Resonance Imaging

Declarations

Ethics approval and consent to participate

The animal study was reviewed and approved by Ethical approval for this study was obtained by the Italian Health Department with authorization n 635/2017.

Consent of publication

Not applicable.

Availability of data and materials

The datasets used and analysed during the current study are available from the corresponding author on reasonable request

Competing interests

The authors declare that they have no competing interests.

Funding

This work has been carried out in the context of the EDEN2020 (Enhanced Delivery Ecosystem for Neurosurgery in 2020) project, that received funding from the European Union's EU Research and Innovation programme Horizon 2020 under Grant Agreement No. 688279.

Authors' contributions

MT developed the quantification method, did the experimentation related to the project, analysed the data, wrote the manuscript and participated in its revision. CS developed the quantification method, analysed the data, wrote the manuscript. AB developed the quantification method, participated in data analysis and revision of the manuscript. DD provided technical support and helped to write the manuscript. LM provided technical support in the experimentation related to the project. AC, VP, AF, MR, LB, GR did the experimentation related to the project, participated in the manuscript revision. SB did the experimentation related to the project, analyzed the data and helped to revise the manuscript. DDZ developed the study design, did the experimentation related to the project, participated in data analysis and helped to revise the manuscript. All the authors have accepted the final version of the manuscript.

References

1. Flecknell P. Replacement, reduction and refinement. *ALTEX*. 2002;19(2):73–8.
2. Janowski M. *Experimental Neurosurgery in Animal Models*. Humana Press; 2016. p. 255.
3. Sun T, Hevner RF. Growth and folding of the mammalian cerebral cortex: from molecules to malformations. *Nat Rev Neurosci*. 2014;15(4):217–32.
4. Russell KN, Mitchell NL, Anderson NG, Bunt CR, Wellby MP, Melzer TR, et al. Computed tomography provides enhanced techniques for longitudinal monitoring of progressive intracranial volume loss associated with regional neurodegeneration in ovine neuronal ceroid lipofuscinoses. *Brain Behav*. 2018;8(9):e01096.
5. Ella A, Delgadillo JA, Chemineau P, Keller M. Computation of a high-resolution MRI 3D stereotaxic atlas of the sheep brain. *Journal of Comparative Neurology*. 2017;525(3):676–92.
6. Pieri V, Trovattelli M, Cadioli M, Zani DD, Brizzola S, Ravasio G, et al. Diffusion Tensor Magnetic Resonance Tractography of the Sheep Brain: An Atlas of the Ovine White Matter Fiber Bundles. *Front Vet Sci*. 2019;6:345.
7. Gerke O, Vilstrup MH, Segtnan EA, Halekoh U, Højlund-Carlsen PF. How to assess intra- and inter-observer agreement with quantitative PET using variance component analysis: a proposal for standardisation. *BMC Med Imaging*. 2016;16(1):54.
8. Bland JM, Altman DG. Measuring agreement in method comparison studies. *Stat Methods Med Res*. 1999;8(2):135–60.
9. Martini L, Fini M, Giavaresi G, Giardino R. Sheep model in orthopedic research: a literature review. *Comp Med*. 2001;51(4):292–9.
10. Dai JX, Ma YB, Le NY, Cao J, Wang Y. Large animal models of traumatic brain injury. *Int J Neurosci*. 2018;128(3):243–54.

11. Karageorgos L, Hein L, Rozaklis T, Adams M, Duplock S, Snel M, et al. Glycosphingolipid analysis in a naturally occurring ovine model of acute neuronopathic Gaucher disease. *Neurobiol Dis.* 2016;91:143–54.
12. Opdam HI, Federico P, Jackson GD, Buchanan J, Abbott DF, Fabinyi GC, et al. A sheep model for the study of focal epilepsy with concurrent intracranial EEG and functional MRI. *Epilepsia.* 2002;43(8):779–87.
13. Boltze J, Förschler A, Nitzsche B, Waldmin D, Hoffmann A, Boltze CM, et al. Permanent middle cerebral artery occlusion in sheep: a novel large animal model of focal cerebral ischemia. *J Cereb Blood Flow Metab.* 2008;28(12):1951–64.
14. Hoffmann A, Stoffel MH, Nitzsche B, Lobsien D, Seeger J, Schneider H, et al. The ovine cerebral venous system: comparative anatomy, visualization, and implications for translational research. *PLoS One.* 2014;9(4):e92990.
15. Hicdonmez T, Parsak T, Cobanoglu S. Simulation of surgery for craniosynostosis: a training model in a fresh cadaveric sheep cranium. Technical note. *J Neurosurg.* 2006;105(2 Suppl):150–2.
16. Grisham W. Resources for teaching Mammalian neuroanatomy using sheep brains: a review. *J Undergrad Neurosci Educ.* 2006;5(1):R1–6.
17. Kamp MA, Knipps J, Steiger HJ, Rapp M, Cornelius JF, Folke-Sabel S, et al. Training for brain tumour resection: a realistic model with easy accessibility. *Acta Neurochir (Wien).* 2015;157(11):1975–81. discussion 81.
18. Damasceno BP. Neuroimaging in normal pressure hydrocephalus. *Dement Neuropsychol.* 2015;9(4):350–5.
19. Laubner S, Ondreka N, Failing K, Kramer M, Schmidt MJ. Magnetic resonance imaging signs of high intraventricular pressure—comparison of findings in dogs with clinically relevant internal hydrocephalus and asymptomatic dogs with ventriculomegaly. *BMC Vet Res.* 2015;11:181.
20. Kolsur N, Shetty PMR, Kumar S AA, editors. Morphometric study of ventricular indices in human brain using computed tomography scans in indian population2018.

Figures

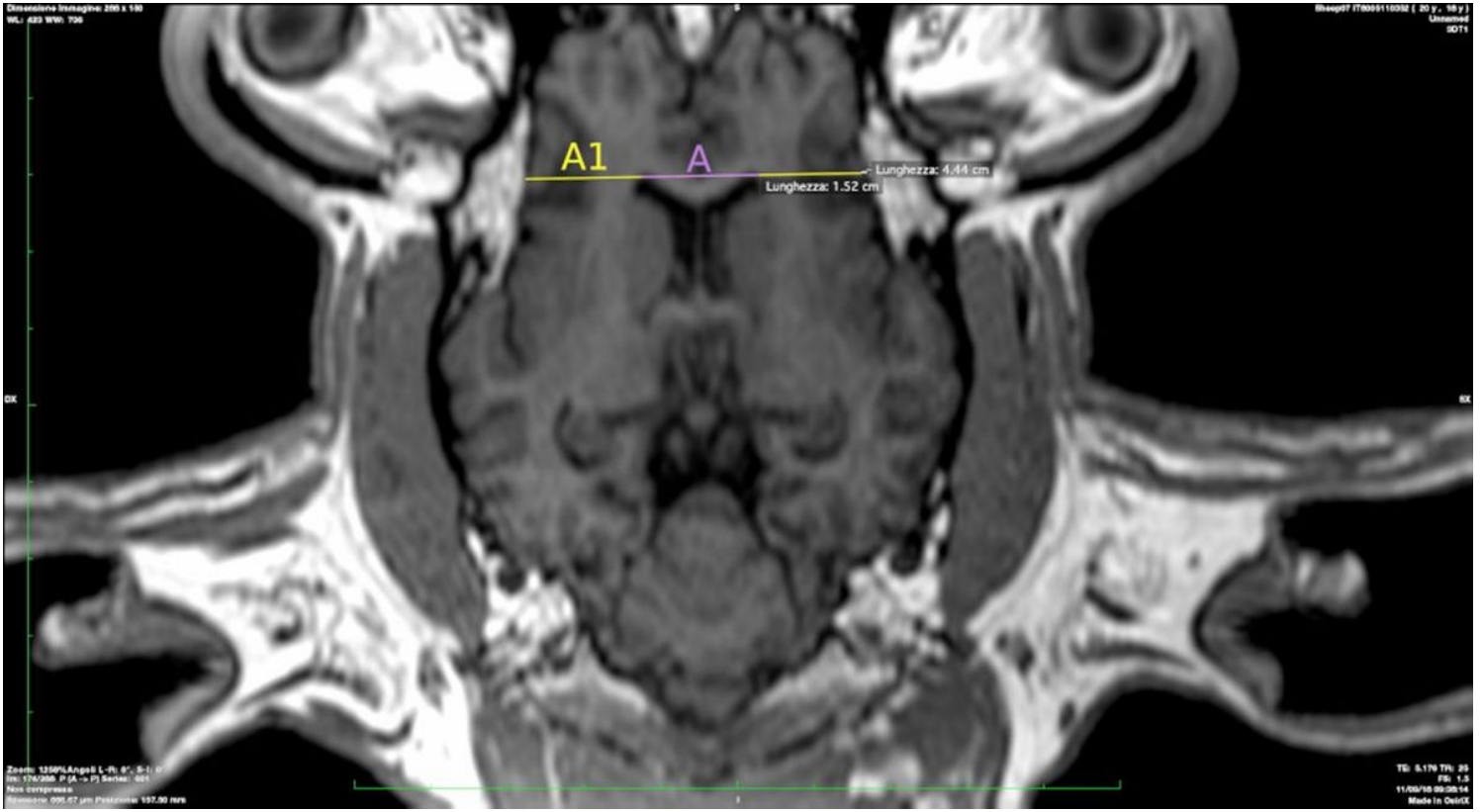


Figure 1

Figure 1



Figure 2

Figure 2

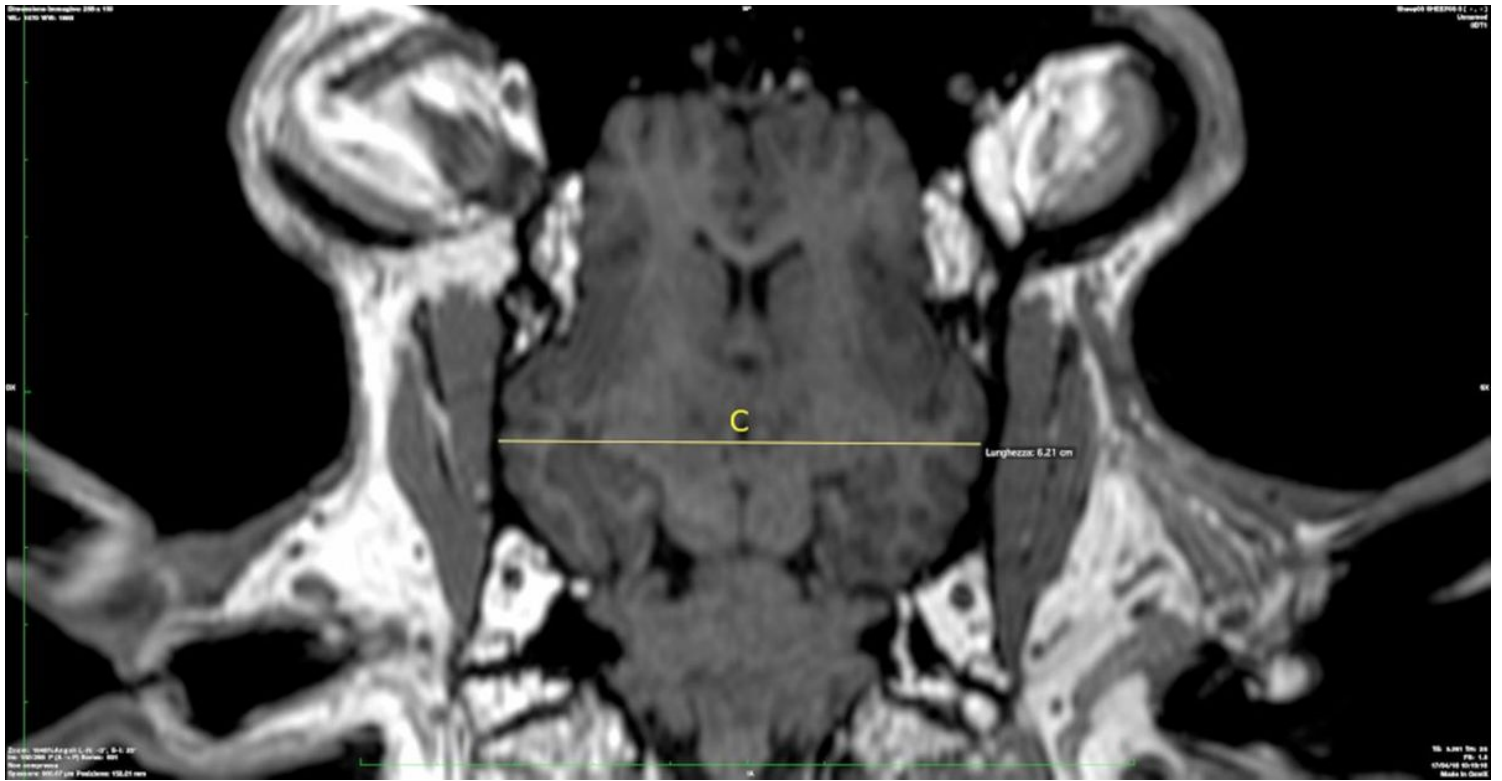


Figure 3

Figure 3

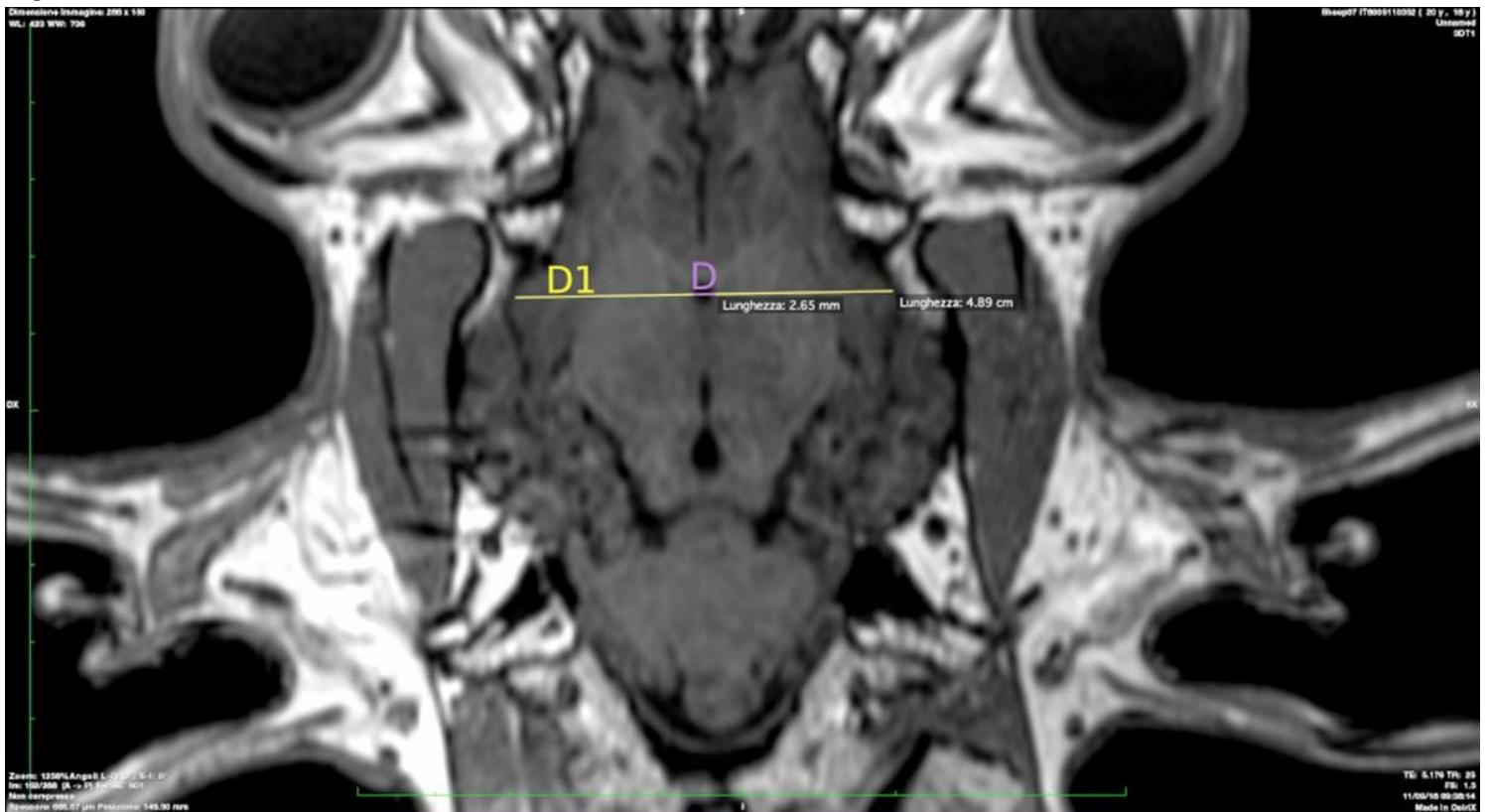


Figure 4

Figure 4

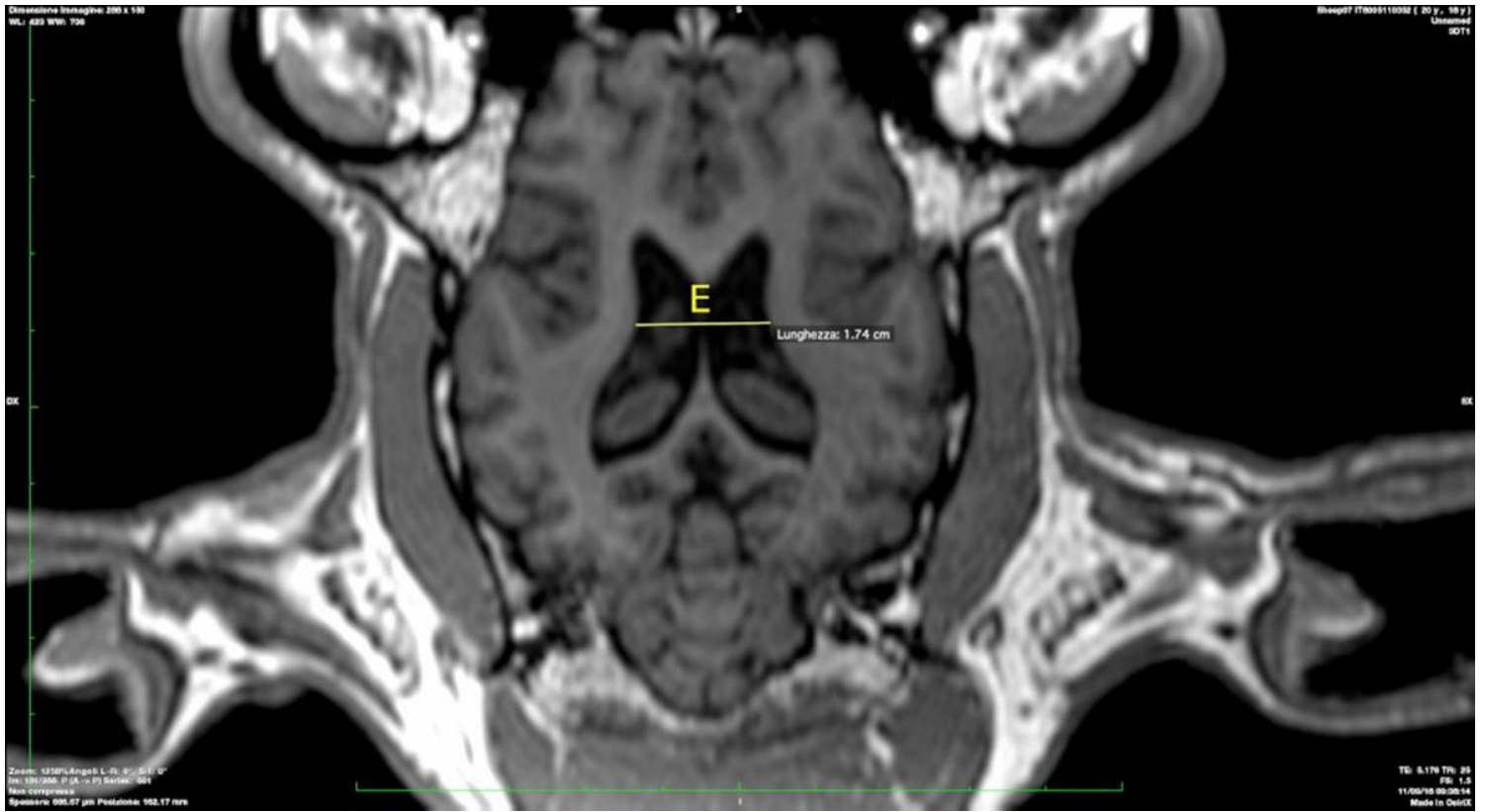


Figure 5

Figure 5

Mean-difference plot of (15 observation pairs): $M_1: A_1$ vs $M_2: B_1$

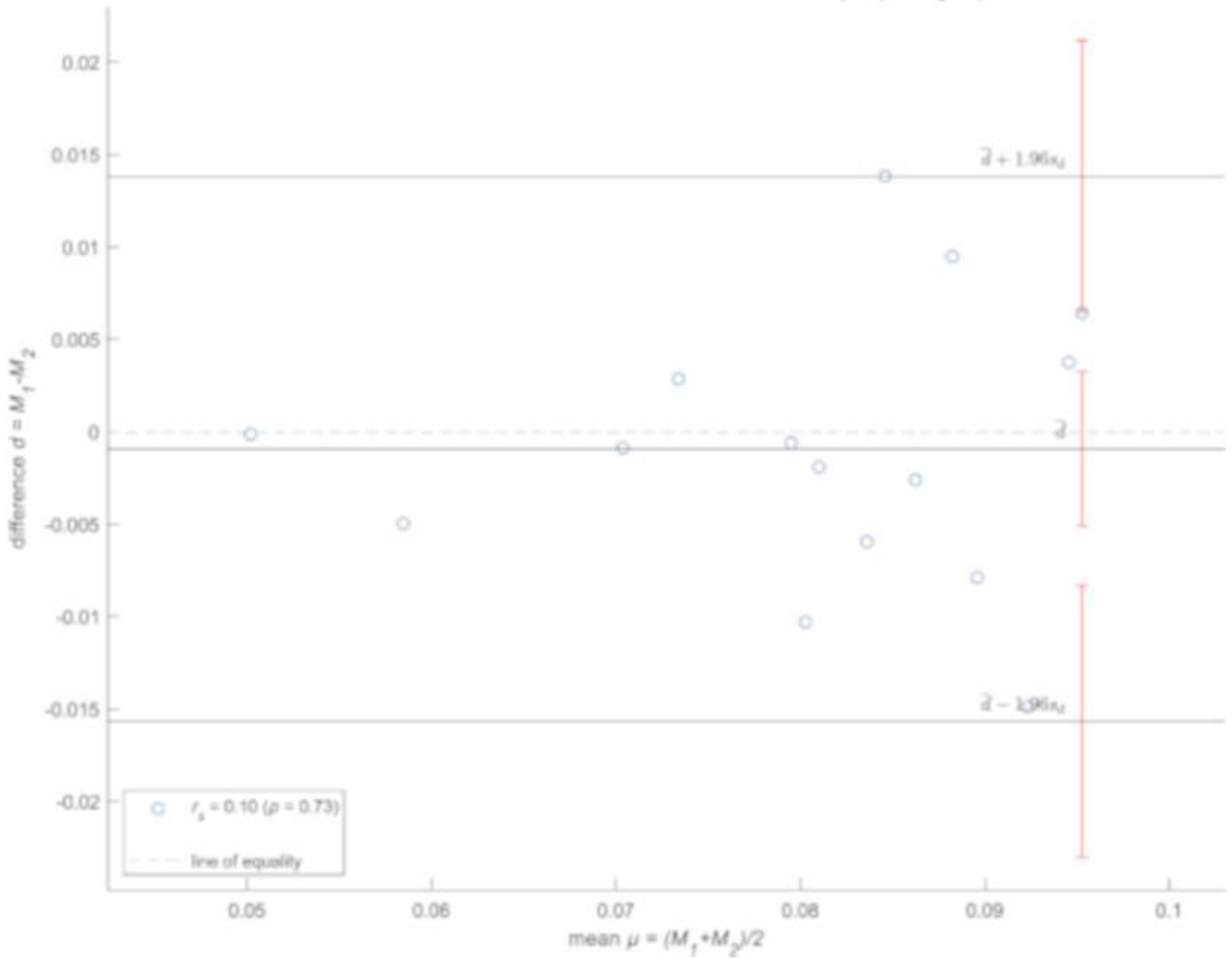


Figure 6

Figure 6